Analysis, Numerical Calculation, Simulation and Experiment of Chaotic Circuits

Yuhao Li* and Yifeng Deng†

School of Physics, Sun Yat-sen University, Guangzhou, Guangdong, China

Date: March 30, 2023

Abstract

We analyzed the stability of Chua's circuit by equilibrium point analysis and lyapunov exponent, and observed the obvious chaotic phenomena such as limit cycle, single attractor and double attractor through numerical calculation, simulation and experiment respectively. In addition, we also analyzed another simple chaotic circuit in the same way and observed some chaotic phenomena, such as double attractors and double periodic bifurcation.

keywords: chaotic phenomena, Chua's circuit, lyapunov exponent, simulation

1 Introduction

Since the meteorologist Lorenz discovered the first chaotic attractor in 1963[1], the research and application of chaos theory have made great progress in the field of nonlinear science. Chaotic motion is extremely sensitive to the initial value, and the extremely small change of the initial value of the system will cause great changes in the oscillation output of the system. With the development of computational science and social science, the unpredictability and regularity of chaos make it a hot research topic in many disciplines such as physics and mathematics.

Chaotic circuit is one of the important ways to study chaos theory. Since Leon O. Chua put forward Chua's circuit in 1983[2], the related research on modified Chua's circuit and chaotic system based on memristor[3] has emerged one after another, and it has been applied to a wider range of fields[4-10]. Under certain parameters, Chua's circuit can produce various rich and complex chaotic dynamic phenomena such as bifurcation, single vortex and double vortex attractor, so it is widely used in chaos experiment teaching.

Since the development of Chua's circuit, there has been a considerable interest in the construction of autonomous chaotic circuits. Often, these modifications involve the

*liyh536@mail2.sysu.edu.cn

†Experiment collaborator

addition of an extra energy storage element such as an inductor at the right place, thereby adding a dimension to a predominantly 2-D limit cycle oscillator. In other cases, notably the Colpits oscillator[11], a chaotic regime is already present for certain values of the design parameters. Others directly translate a known chaotic system of differential equations to electronics. The necessary nonlinear terms are implemented by using dedicated analog multipliers as in[12] or operational-amplifier-based piecewise continuous functions[13].

However, a very simple chaotic circuit was proposed in 2015 based on modifying the Resistor-Capacitor phase shift oscillator[14]. This circuit does not need dedicated nonlinear elements, and the operation does not depend on the dynamic properties of the active components. Neither the component values nor the supply voltage is critical. Additionally, the circuit has the attractive feature that the underlying core oscillator is clearly visible in the structure. This makes it a great introductory pedagogical tool for students interested in chaos.

Here, we analyze the dynamics of Chua's circuit, and discuss the regular contained in chaos through stability analysis and calculation of Lyapunov exponent. We observed Chua's circuit in three ways: numerical calculation, circuit simulation and experiment, and all of them observed obvious chaotic phenomena such as limit cycle, single attractor and double attractor. In addition, we also observed the simple chaotic circuit mentioned above and made some analysis.

2 Chaotic circuit model and its dynamic analysis

2.1 The normalized equations of Chua's circuit

A typical Chua's circuit is shown in Fig.1. The circuit consists of a inductor L, two capacitors C_1 and C_2, a linear resistor R_1 and a nonlinear resistor R_N. The inductor L and capacitor C_2 form an LC oscillation circuit; the nonlinear resistor R_N is connected in parallel with capacitor C_1 in a filter circuit to phase shift the sinusoidal signal generated by the oscillator; the resistor R_1 regulates the phase difference between C_1 and C_2 and consumes energy. The whole circuit can be described by the following equations:

$$\frac{\mathrm{d}U_{C_1}}{\mathrm{d}t} = \frac{1}{R_1 C_1}\left(U_{C_2} - U_{C_1}\right) - \frac{1}{C_1} f\left(U_{R_N}\right) \tag{1a}$$

$$\frac{\mathrm{d}U_{C_2}}{\mathrm{d}t} = \frac{i_L}{C_2} + \frac{1}{R_1 C_2}\left(U_{C_1} - U_{C_2}\right) \tag{1b}$$

$$\frac{\mathrm{d}i_L}{\mathrm{d}t} = -\frac{1}{L} U_{C_2} \tag{1c}$$

$$f\left(U_{R_N}\right) = G_b U_{C_1} + \frac{1}{2}\left(G_a - G_b\right)\left(\left|U_{C_1} + E\right| - \left|U_{C_1} - E\right|\right) \tag{1d}$$

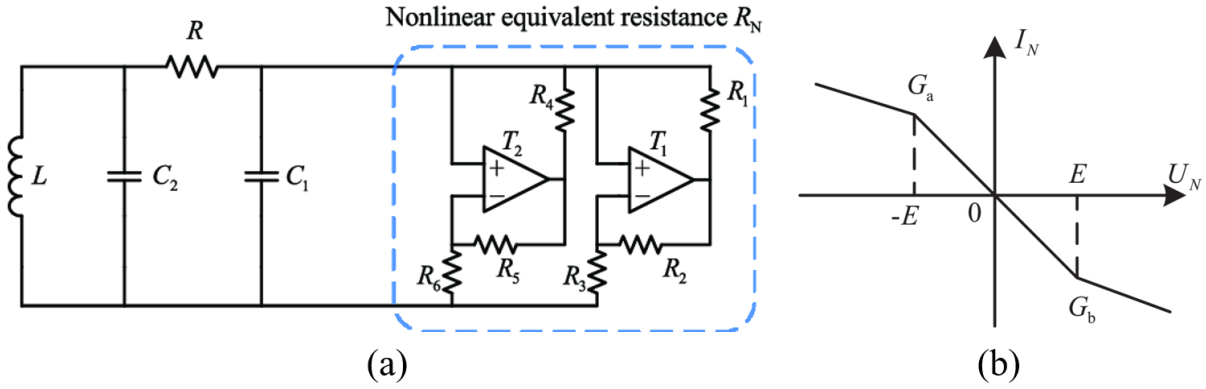

Fig. 1: Diagram of a typical Chua's circuit.
Fig (a): Circuit diagram of a typical Chua's circuit. The inductor L, capacitors C_1 and C_2, and resistor R_1 are all linear components, and R_N is an active nonlinear resistor. A common structure of realizing R_N by two triodes and some resistors has been drawn on the figure. Fig (b): Volt-ampere characteristic curve of nonlinear resistor R_N.
Source: Both pictures are from paper[15].

Among them, G_a is the conductance of the inner interval, G_b is the conductance of the outer interval, and E is the voltage of the turning point of the inner and outer interval.

Using Eq.(1) to discuss the dynamics of the circuit is troublesome. Let $x = U_1/E$, $y = U_2/E, z = Ri_L/E$, $a = RG_a$, $b = RG_b$, $\alpha = C_2/C_1$, $\beta = R^2C_2/L$, then the equations can become a normalized and dimensionless system of nonlinear equations:[1]

$$\begin{cases} \dot{x} = \alpha(y - x - f(x)) \\ \dot{y} = x - y + z \\ \dot{z} = -\beta y \\ f(x) = bx + \frac{1}{2}(a - b)(|x + 1| - |x - 1|) \end{cases} \tag{2}$$

According to Eq(2), we can easily carry out numerical calculation based on MATLAB (see **Appendix B.1** for the code of numerical calculation). According to the component parameters of the actual circuit, we take $a = -1.2768, b = -0.6888$, keep $\alpha = 8$ unchanged, and get different chaotic phenomena when β takes different values (as shown in Fig.2). Note that in order to get the left single attractor and the right single attractor, we need to set different initial conditions, which have been marked in the illustration, and other images that are not marked have adopted initial values $x_0, y_0, z_0 = (1, 0, 0)$.

Generally speaking, with the increase of β, that is, the increase of R in the circuit, we will observe straight lines, limit cycles, double attractors and single attractors (left or

[1]Here I have to point out a typo in our lab lectures: in the third lecture of this experiment, the first formula of Eq.(2) is written as $\dot{x} = \alpha(y - x) - f(x)$.

right, depending on the initial conditions and symmetry of the circuit) in turn.

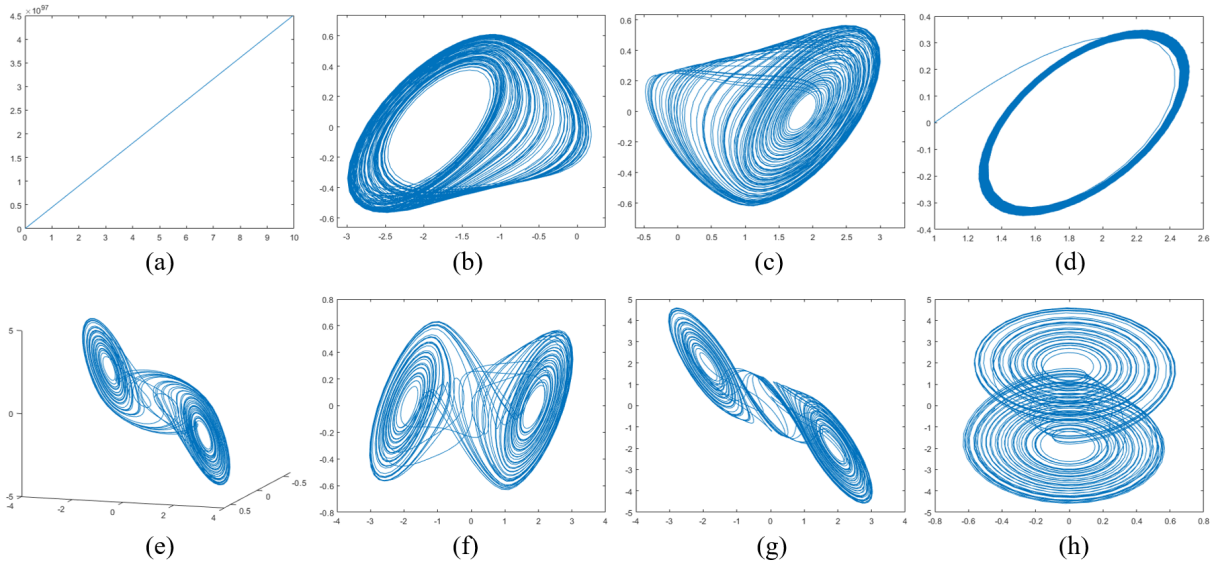

Fig. 2: numerical calculation of normalized Chua's circuit equations.
(a) straight line, $\beta = 0.1$ (b) left single attractor, initial value $x_0, y_0, z_0 = (-1, 0, 0)$ and $\beta = 14.7$ (c) right single attractor, initial value $x_0, y_0, z_0 = (1, 0, 0)$ and $\beta = 14.7$ (d) limit cycle, $\beta = 19.35$ (e) three-dimensional double attractor, $\beta = 13.6$ (f) projection of double attractor on xy plane (g) projection of double attractor on xz plane (h) projection of double attractor on yz plane.

2.2 Stability analysis of equilibrium point and timing diagram

From Eq(2), we can see that the nonlinear term of the Chua's circuit equation is a segmented linear function, so we can divide the phase space into three linear regions for analysis, which are

$$\begin{cases} D_1 = \{(x, y, z) \mid x > 1\} \\ D_0 = \{(x, y, z) \mid -1 \leq x \leq 1\} \\ D_{-1} = \{(x, y, z) \mid x < -1\} \end{cases} \tag{3}$$

Let $\dot{x} = 0, \dot{y} = 0, \dot{z} = 0$, we can get three equilibrium points as

$$\begin{cases} P^+ = (1.89, 0, -1.89) \in D_1 \\ P^0 = (0, 0, 0) \in D_0 \\ P^- = (-1.89, 0, 1.89) \in D_{-1} \end{cases} \tag{4}$$

Fig.3 shows the timing diagrams of x, y, and z for $\beta = 12.25$ and $\beta = 20$. $\beta = 12.25$ is a double attractor, and it can be seen that x and z oscillate between the equilibrium points of 1.89 and -1.89, and y oscillates around the equilibrium point 0. for $\beta = 20$, x, y, and z oscillate around their first equilibrium point, respectively.

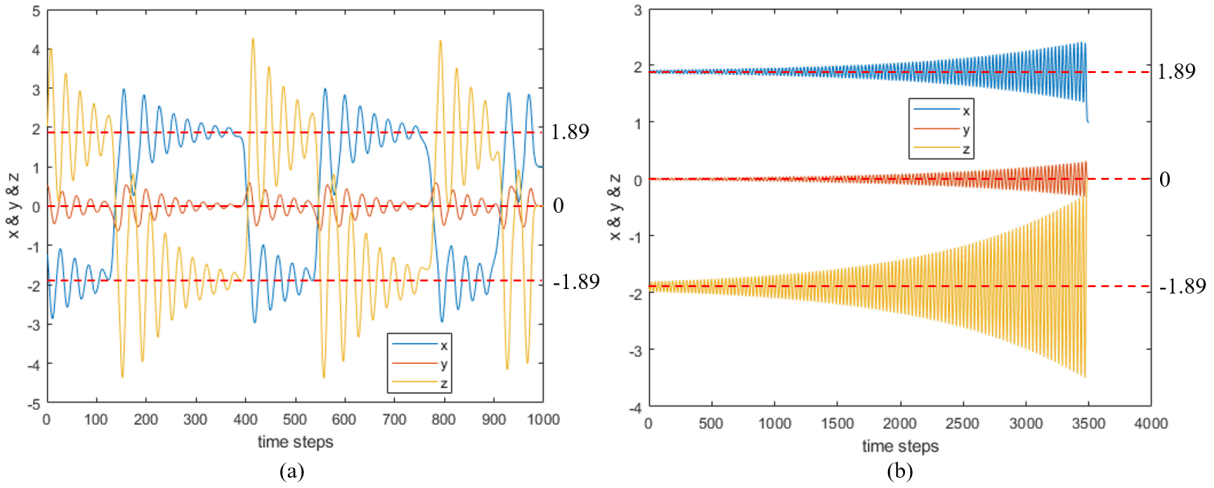

Fig. 3: Timing diagrams of x, y, and z. (a) $\beta = 12.25$ (b) $\beta = 20$.
x, y, and z oscillate around the expected equilibrium point for different values of β, and x and z oscillate in opposite positions, which is also consistent with the results expected from Eq.(4)

We also observe the timing diagrams when the β is very small and very large. x, y and z converge to the equilibrium point 0 when $\beta < 9.85$, while they oscillate around 1.89, 0, and -1.89 when $\beta > 15.21$, respectively.

A more detailed analysis[16] shows that the equilibrium points P+ and P- are the saddle focal points of index 2. P^+ and P^- themselves consist of a stable component pointing axially toward the equilibrium point and an unstable component leaving the equilibrium point radially. The joint action of these two components of motion causes their phase trajectories to form a radially expanding and axially contracting spiral motion. Since the speed of radial expansion is much smaller than the speed of axial contraction, a vortex coil is formed. The equilibrium point P^0 is the saddle focus of index 1, which consists of the unstable component leaving the equilibrium point in the axial direction and the stable component pointing to the equilibrium point in the radial direction. The joint action of these two motion components makes its phase trajectory form a spiral motion of radial contraction and axial expansion. Since the speed of radial contraction is much smaller than that of axial expansion, the bond band is formed as the radius of the spiral tends to zero as time increases.

When $9.95 < \beta < 10.34$, assuming that the initial position of the phase trajectory is in the D_1 region, an outwardly expanding vortex will be formed in the D_1 region, and with the increasing radius of the vortex, when the trajectory reaches the critical plane, it will cross the plane into the D_0 region, form a bond band in the D_0 region, and cross another critical plane and enter the D_2 region to form the vortex, and then from the

D_0 region through the above Then, the vortex enters the D_1 region through the above process, and the double vortex attractor is formed in this way. (see Fig.4(a))

However, when $10.34 < \beta < 15.21$, the initial position of the phase trajectory is in D_1 region, and the vortex will be expanded outward in D_1 region, but with the increasing radius of the vortex, when the trajectory reaches the critical plane, it will not cross the critical plane, but will be turned back and return to D_1 region again, and so on, forming a single vortex attractor. (see Fig.4(b))

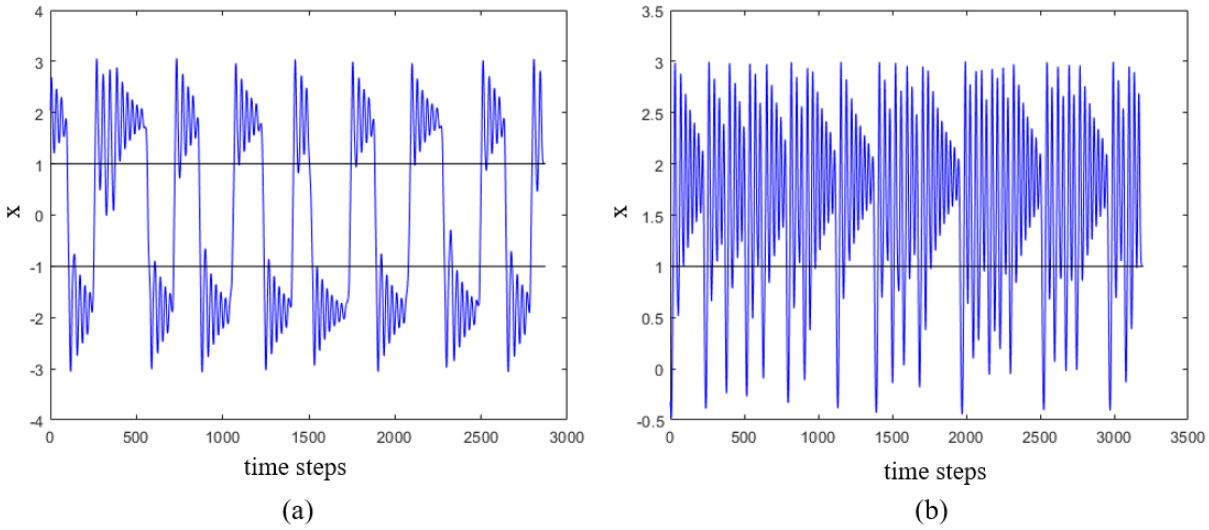

Fig. 4: Timing diagram of x (a) double attractor (b) single attractor

The black solid line in the figure divides the different regions according to Eq.(3). For the case of double attractor, x makes vortex motion in the D_1 and D_{-1} regions, respectively, and crosses the D_0 region in a straight line. For the case of single attractor, when x leaves the initial region (D_1 or D_{-1}) it immediately bends back and returns to the original region again. This explains why we can only find one of the left single attractor or right single attractor in the experiments and simulations.

2.3 Lyapunov exponential spectrum and chaos

Lyapunov exponent[17-19] is a powerful tool to analyze chaos. It can judge whether the two tracks will overlap or the gap will become wider in the following time by giving a certain small disturbance to the initial value and then calculating the distance between the two tracks. If the largest Lyapunov exponent is positive, it shows that the evolution of the system will be different when the initial values are very different, that is, chaos phenomenon. We use MATLAB to calculate the lyapunov exponent spectrum about β, as shown in Fig.5, and the related code can be found in the **Appendix B.2**.

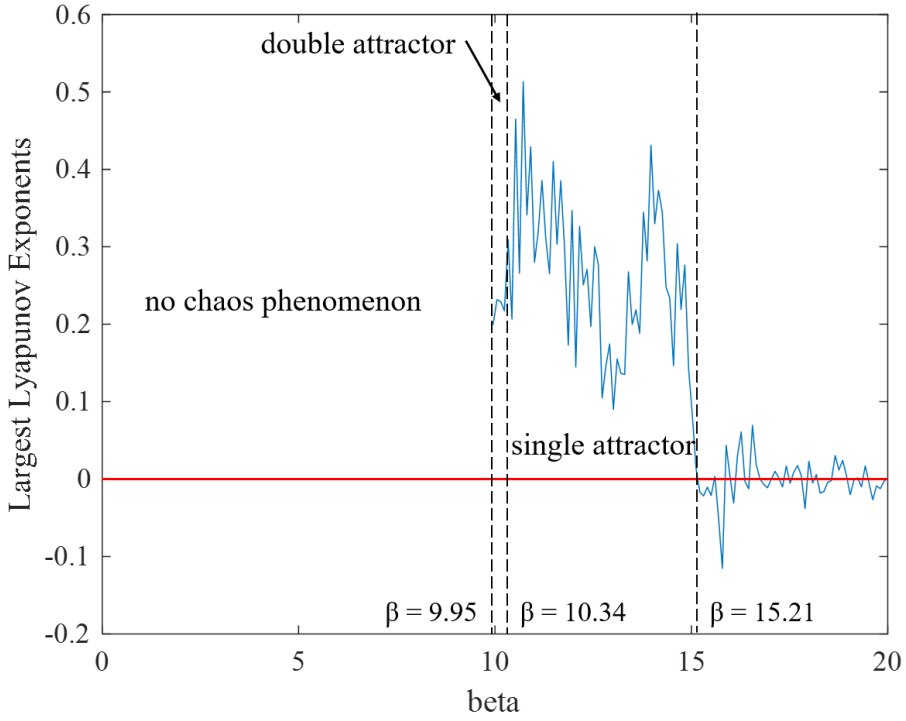

Fig. 5: Lyapunov exponent spectrum of normalized Chua's circuit about parameter β.

$\beta = 9.95, \beta = 10.34$ and $\beta = 15.21$ divide Fig.5 into four regions. The first area is before the double attractor is observed. At this time, there is no chaos phenomenon and no positive lyapunov exponent in the circuit. The second small region is a double attractor, followed by single attractor, and finally an unstable region, where limit cycles sometimes appear.

Fig.5 clearly corresponds to the different phenomena in Fig.2, and tells us when chaos will occur and when mutation will occur. More interestingly, we can see that the lyapunov exponent in Fig.5 is not a smooth curve, but very tortuous. This is related to a phenomenon that we accidentally found when tuning parameters: the circuit is unstable in the state of double attractor and single attractor, and the circuit will oscillate between the state of double attractor and single attractor when the β of different orders of magnitude changes, which is a bit like some kind of self-similarity. Related discussions can be found in the **Appendix A.1**.

3 Circuit simulation and experiment

We use Multisim to simulate Chua's circuit according to Fig.6, and do experiments according to the same circuit diagram. The comparison between simulation and experiment is shown in Fig.7.

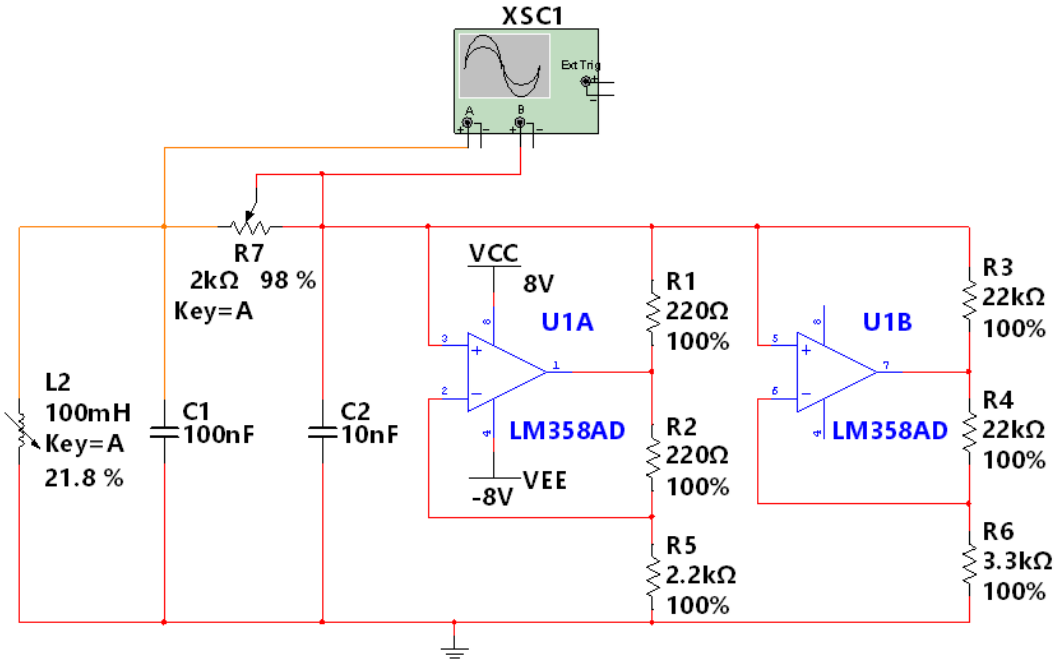

Fig. 6: The circuit diagram used in the simulation. The parameters of components have been marked in the diagram. The same circuit diagram was used in the experiment.

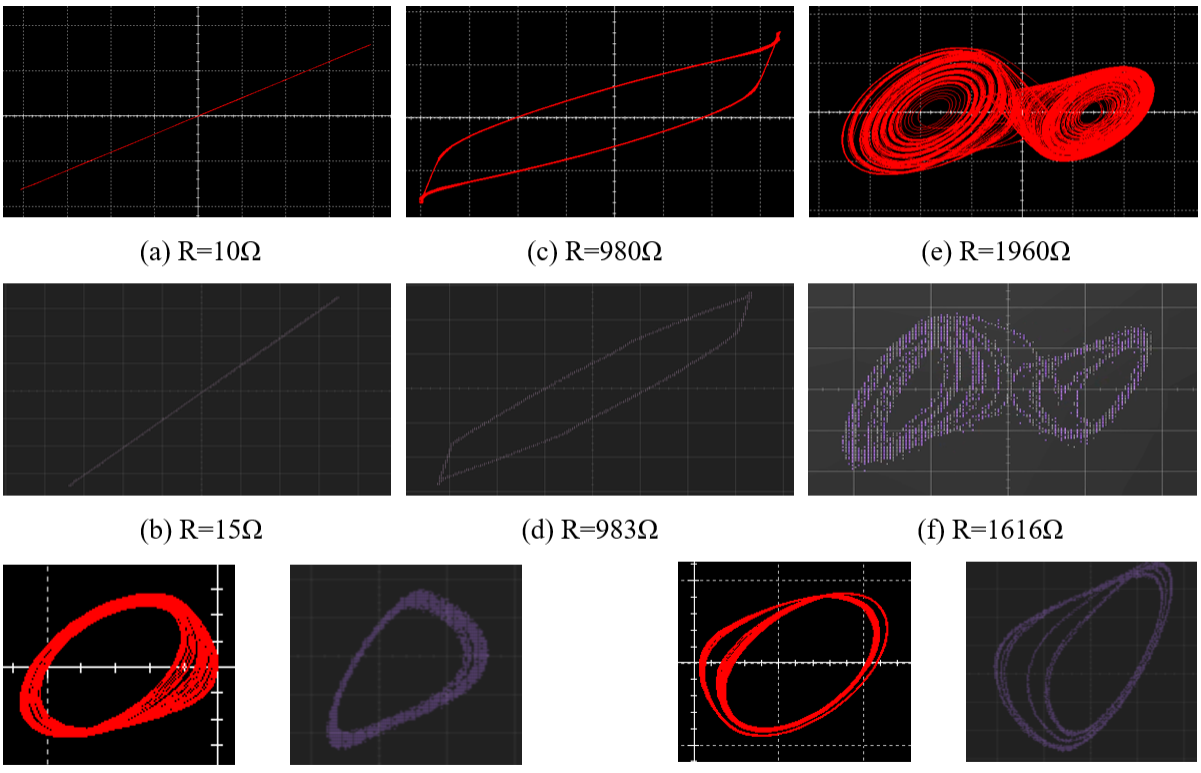

(a) R=10Ω (c) R=980Ω (e) R=1960Ω

(b) R=15Ω (d) R=983Ω (f) R=1616Ω

(g) R=1880Ω (h) R=1808Ω (i) R=1428Ω (j) R=1389Ω

Fig. 7: Comparison between simulation and experiment. The value of R_7 corresponding to each picture has been marked at the bottom of the picture. The red line is the simulation result, and the purple line is the experimental result. In order to see more clearly, we adjusted the contrast and sharpness of the experimental screenshots.

In this circuit, two operational amplifiers (the right half of the circuit diagram) are used as nonlinear terms. We can see that the two phenomena of straight line and limit cycle are in good agreement with each other in experiment and simulation. However, there are some differences between the values of R_7 in the simulation and experiment of double attractor and single attractor. And in the experiment, our circuit prefers the left single attractor, but it is difficult to call out the right single attractor. In Sec.2, we have found that this is related to the initial conditions of the circuit. Moreover, because the resistance of each resistor is not completely accurate in the experiment, the symmetry of the circuit is also deviated.

4 Simple two-transistor resistor-capacitor chaotic oscillator

We choose a two-transistor resistor-capacitor chaotic circuit[14] to do similar analysis, numerical calculation, simulation and experiment again. The circuit is shown in Fig.8. This circuit includes a transistor-based RC oscillator to which a small subcircuit is added, directly interacting with the RC ladder itself. The purpose of the subcircuit is to add a nonlinearity in the RC ladder.

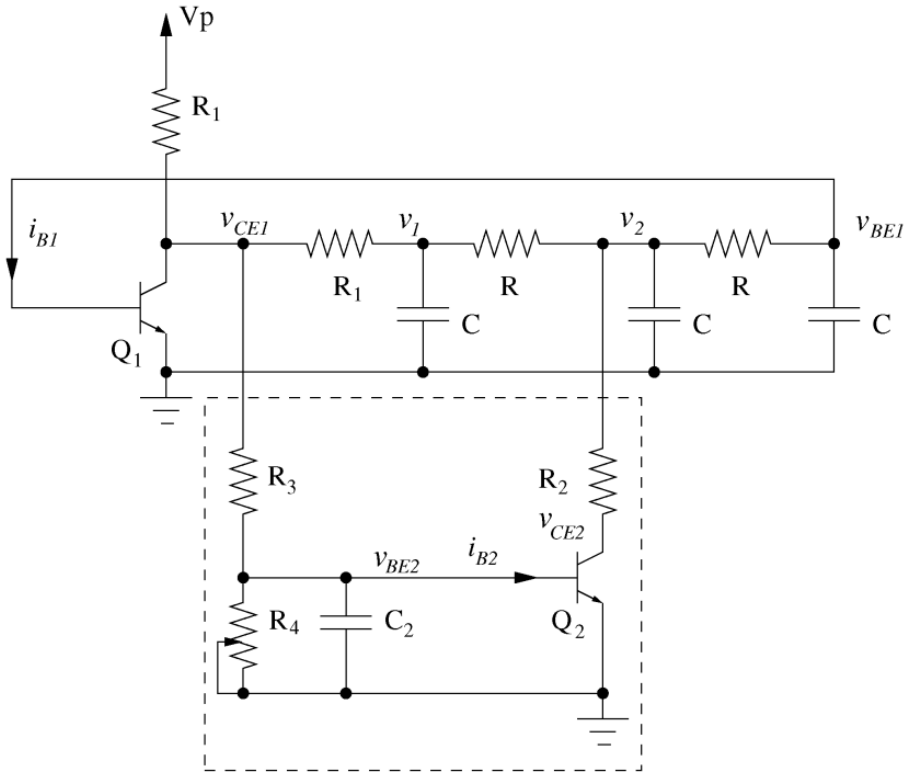

Fig. 8: Circuit diagram of the two-transistor resistor-capacitor chaotic oscillator.
$R = 10\text{k}\Omega, R_1 = 5\text{k}\Omega, R_2 = 15\text{k}\Omega, R_3 = 30\text{k}\Omega$, $C = 1\text{nF}, C_2 = 360\text{pF}$, and $V_p = 5$ V

$$RC\frac{\mathrm{d}v_1}{\mathrm{d}t} = -v_1\left(1+\frac{R}{R_1}-\frac{RR_3}{R_1\left(2R_3+R_1\right)}\right)+v_2+\frac{RR_3}{2R_3+R_1}\left(\frac{V_p}{R_1}-i_{C1}+\frac{v_{BE2}}{R_3}\right) \tag{5a}$$

$$RC\frac{\mathrm{d}v_2}{\mathrm{d}t} = -2v_2+v_1+v_{BE1}-i_{C2}R \tag{5b}$$

$$RC\frac{\mathrm{d}v_{BE1}}{\mathrm{d}t} = -v_{BE1}+v_2-i_{B1}R \tag{5c}$$

$$\left(2R_3+R_1\right)C_2\frac{\mathrm{d}v_{BE2}}{\mathrm{d}t} = -v_{BE2}\left(2+\frac{2R_3+R_1}{R_4}\right)+v_1+V_p-i_{C1}R_1-i_{B2}\left(2R_3+R_1\right) \tag{5d}$$

We simplify the circuit model and normalize it to get (see **Appendix A.2** for detailed discussion and derivation of simplification)

$$\begin{aligned}
\dot{x} &= -2x-1+y+a-h_\alpha(z,1+a+x)\\
\dot{y} &= -2y+x+z-h_\beta(u,2/3(y+1))\\
\dot{z} &= -z+y\\
\tau\dot{u} &= -ub-b+\frac{a}{2}+\frac{1}{2}+\frac{x}{2}-\frac{1}{2}h_\alpha(z,1+a+x)
\end{aligned} \tag{6}$$

Where $a=25/3, b=1+R3/R4,\ =80,\ =10a=25/3,\ b=1+R_3/R_4,\ \alpha=80,\ \beta=10,$ and h is defined as

$$h_\gamma(x,y)=\begin{cases}\min(\gamma x,y) & ,x>0\\ 0 & ,x\le 0\end{cases} \tag{7}$$

We use MATLAB to calculate Eq.(6) numerically. The related code can be found in **Appendix B.3**. The whole system is four-dimensional, so we can't show its phase space intuitively. We choose some good three-dimensional and two-dimensional "projections" to try to show the general shape of their phase space, as shown in Fig.1010.

A more intuitive and wonderful way is to observe the phase trajectory in $v_1-v_{CE1}-v_{CE2}$ space. We didn't successfully get this image by numerical calculation, but the researchers in paper[14] got a good image by SPICE simulation, as shown in Fig.9.

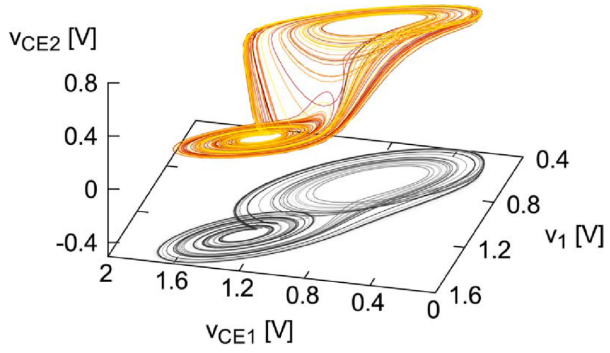

Fig. 9: Three-dimensional view of the attractor in $v_1-v_{CE1}-v_{CE2}$ space.[14]

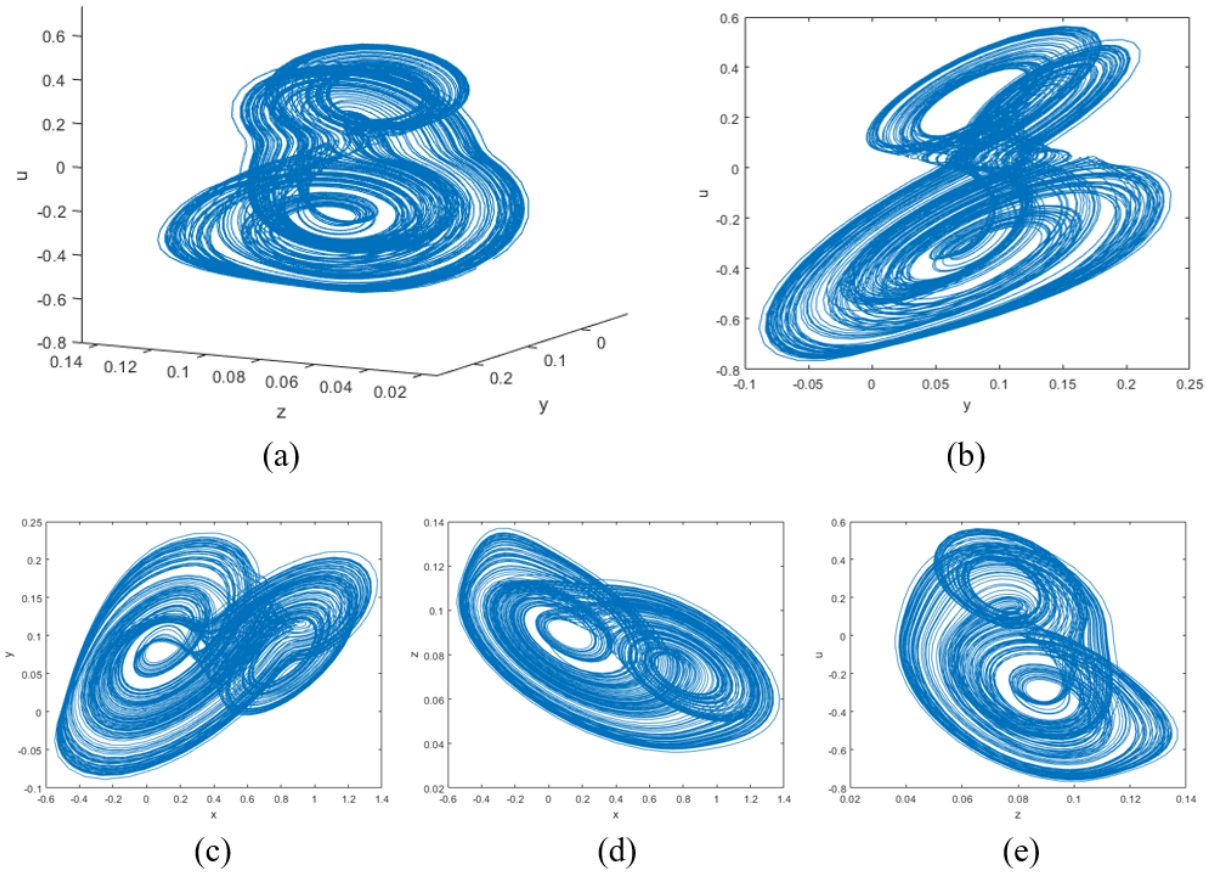

Fig. 10: Multi-angle projection of system phase space. $b = 1.6818$, which is a double attractor state. (a) projection of four-dimensional phase space in zyu space; (b) projection in yu plane; (c) projection in xy plane; (d) projection in xz plane; (e) projection in zu plane.

Then we carried out simulation and experiment, and the circuit diagrams used are shown in Fig.11. Note that we have exchanged the roles of R_7 and R_5. In Fig.8, the upper component is a constant resistor and the lower component is a sliding rheostat, but in Fig.11, they are exchanged.

It is estimated that the main oscillation frequency of this circuit is 44kHz, which is so high that it is difficult to observe all clear phenomena in experiments and simulations. Another difference is that we v_{CE1} as an observation point in both simulation and experiment, but we failed to solve this variable in numerical calculation. Therefore, our experiments and simulations can only roughly verify some obvious chaotic phenomena. Fig.12 shows the limit cycle, double period bifurcation and multiple period bifurcation of the circuit with the change of resistance. Fig.13 shows the state that the circuit has double attractors.

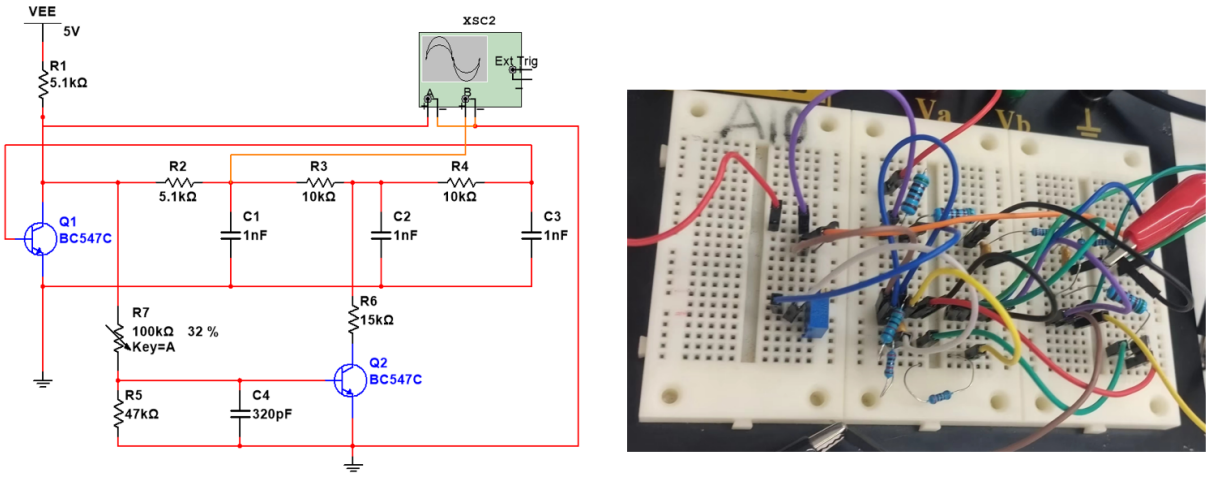

Fig. 11: (a) Circuit diagram of simulation; (b) Circuit diagram of experiment (Although it is a difficult task to identify a complete circuit from it.)

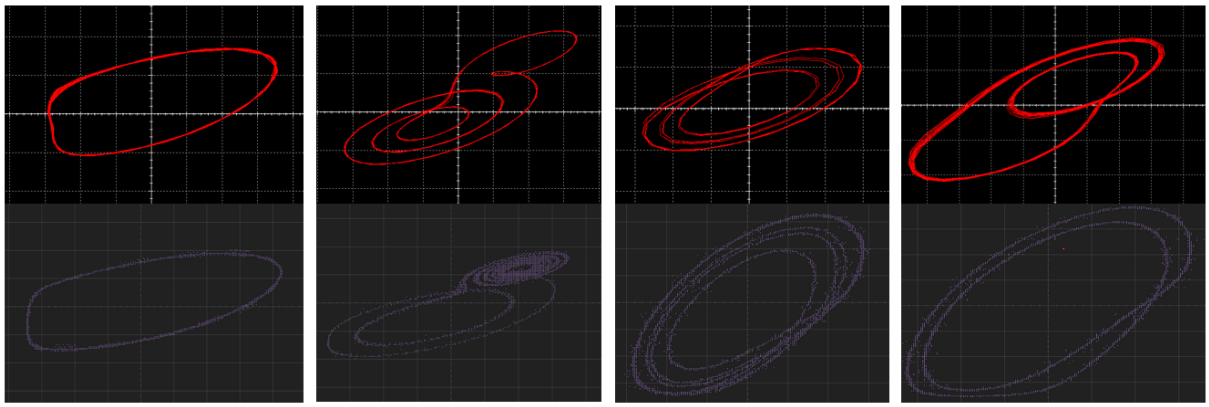

Fig. 12: (a) limit cycle; (b)critical state (about to enter the double attractor); (c)multiple period bifurcation; (d) double period bifurcation. The simulation is above, and the experiment is below.

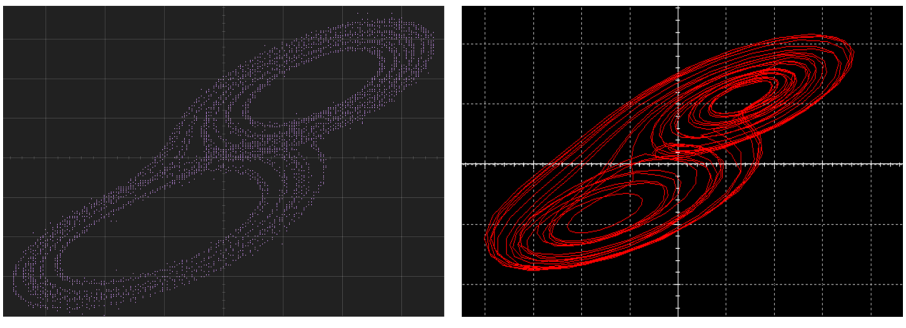

Fig. 13: The state that the circuit has double attractors (a) experiment (b) simulation

5 Conclusion and discussion

Firstly, we analyze the equilibrium point and its stability of the normalized Chua's equation, verify the equilibrium point with the timing diagram, and explain the causes of single attractor and double attractor. Then we draw the largest lyapunov exponent spectrum of Chua's circuit, and intuitively show the chaotic phenomenon in different intervals of β. We observed the chaotic phenomena of Chua's circuit by numerical calculation, simulation and experiment, including limit cycle, single attractor and double attractor.

We also analyze the two-transistor resistor-capacitor chaotic circuit, which is a fourth-order autonomous hyperchaotic system. The dimensionless normalized equation is obtained by simplifying the model, and then we observe the projection of phase space in different dimensions and angles through numerical calculation, simulation and experiment. The obvious chaotic phenomena of this circuit are limit cycle, double attractor, single and multiple periodic bifurcation (only observed in simulation).

There are still some questions for further study. We found in simulation and experiment that when adjusting the resistance, the circuit will have an effect similar to "hysteresis loop", that is, firstly adjust the resistance value of the resistor to a larger value, and then adjust back to the original value, and the circuit state will be different. We suspect that this is caused by nonlinear components such as operational amplifier, capacitor or transistor, but what factors are related to it needs further exploration.

Acknowledgments

We wish to acknowledge Mr. Shen Han and Mr. Liao Deju for their careful guidance in the experiment. And we also thank Tang Bei and Peng Jiahua for their help and discussion in the experiment.

References

[1] LORENZ E N. Deterministic nonperiodic flow[J]. Journal of atmospheric sciences, 1963, 20(2): 130-141.

[2] CHUA L. Memristor-the missing circuit element[J]. IEEE Transactions on circuit theory, 1971, 18(5): 507-519.

[3] STRUKOV D B, SNIDER G S, STEWART D R, et al. The missing memristor found[J]. nature, 2008, 453(7191): 80-83.

[4] LIU S, WANG Y, FARDAD M, et al. A memristor-based optimization framework for artificial intelligence applications[J]. IEEE Circuits and Systems Magazine, 2018, 18(1): 29-44.

[5] WANG H, YE J M, MIAO Z H, et al. Robust finite-time chaos synchronization of time-delay chaotic systems and its application in secure communication[J]. Transactions of the Institute of Measurement and Control, 2018, 40(4): 1177-1187.

[6] SONG H, KIM Y S, PARK J, et al. Designed memristor circuit for self-limited analog switching and its application to a memristive neural network[J]. Advanced Electronic Materials, 2019, 5(6): 1800740.

[7] YANG J Q, WANG R, WANG Z P, et al. Leaky integrate-and-fire neurons based on perovskite memristor for spiking neural networks[J]. Nano Energy, 2020, 74: 104828.

[8] KIM K M, WILLIAMS R S. A family of stateful memristor gates for complete cascading logic[J]. IEEE Transactions on Circuits and Systems I: Regular Papers, 2019, 66(11): 4348-4355.

[9] LASTRAS-MONTANO M A, CHENG K T. Resistive random-access memory based on ratioed memristors[J]. Nature Electronics, 2018, 1(8): 466-472.

[10] BAO B, WANG N, XU Q, et al. A simple third-order memristive band pass filter chaotic circuit[J]. IEEE Transactions on Circuits and Systems II: Express Briefs, 2016, 64(8): 977-981.

[11] KENNEDY M P. Chaos in the colpitts oscillator[J]. IEEE Transactions on Circuits and Systems I: Fundamental Theory and Applications, 1994, 41(11): 771-774.

[12] KINGNI S T, KEUNINCKX L, WOAFO P, et al. Dissipative chaos, shilnikov chaos and bursting oscillations in a three-dimensional autonomous system: theory and electronic implementation[J]. Nonlinear Dynamics, 2013, 73: 1111-1123.

[13] SPROTT J C. A new class of chaotic circuit[J]. Physics Letters A, 2000, 266(1): 19-23.

[14] KEUNINCKX L, VAN DER SANDE G, DANCKAERT J. Simple two-transistor single-supply resistor–capacitor chaotic oscillator[J/OL]. IEEE Transactions on Circuits and Systems II: Express Briefs, 2015, 62(9): 891-895. DOI: 10.1109/TCSII.2015.2435211.

[15] CHEN Y, JIANG W, ZHENG Y, et al. Emi suppression of high-frequency isolated quasi z-source inverter based on multi-scroll chaotic pwm modulation[J/OL]. IEEE Access, 2019, 7: 146198-146208. DOI: 10.1109/ACCESS.2019.2946233.

[16] LAVRÖD J. The anatomy of the chua circuit[Z]. 2014.

[17] NARVAEZ D M D, MESA F, ALZATE P P C. Lyapunov exponents analysis and phase space reconstruction to chua' s circuit[J]. Contemporary Engineering Sciences, 2018, 11: 50.

[18] MEADOR C E E. Numerical calculation of lyapunov exponents for three-dimensional systems of ordinary differential equations[Z]. 2011.

[19] KARABUTOV N. Structural methods of estimation lyapunov exponents linear dynamic system[J]. International journal of intelligent systems and applications, 2015, 7(10): 1-11.

[20] KEUNINCKX L, VAN DER SANDE G, DANCKAERT J. A simple two-transistor chaos generator based on a resistor-capacitor phase shift oscillator[J]. IEICE Proceedings Series, 2014, 46(C2L-A4).

Appendix A Supplementary material

A.1 State oscillation and self-similarity in Chua's circuit

Fig.5 shows that the circuit will change from a double attractor to a single attractor when β is around 10.34. However, we find that this transition is not like "phase transition". Once it reaches a certain critical value, it has always been a single attractor, and before that it will always be a double attractor. Instead, our simulation experiment shows that Chua's circuit will oscillate between these two States, even if beta is accurate to a very low order of magnitude.

Fig.14∼17 show the oscillates between single attractor and double attractor when β is accurate to different orders of magnitude.

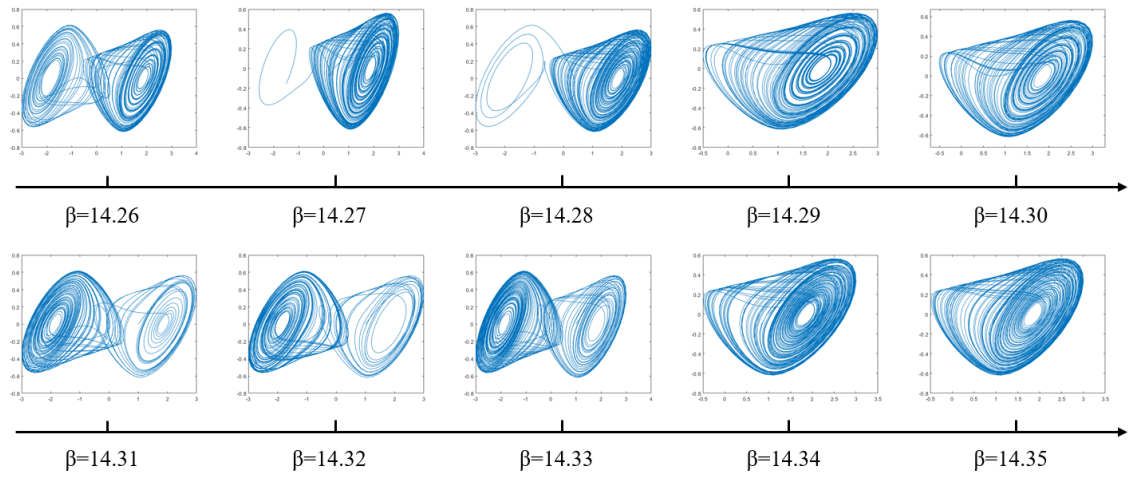

Fig. 14: $\beta \sim 10^{-2}$

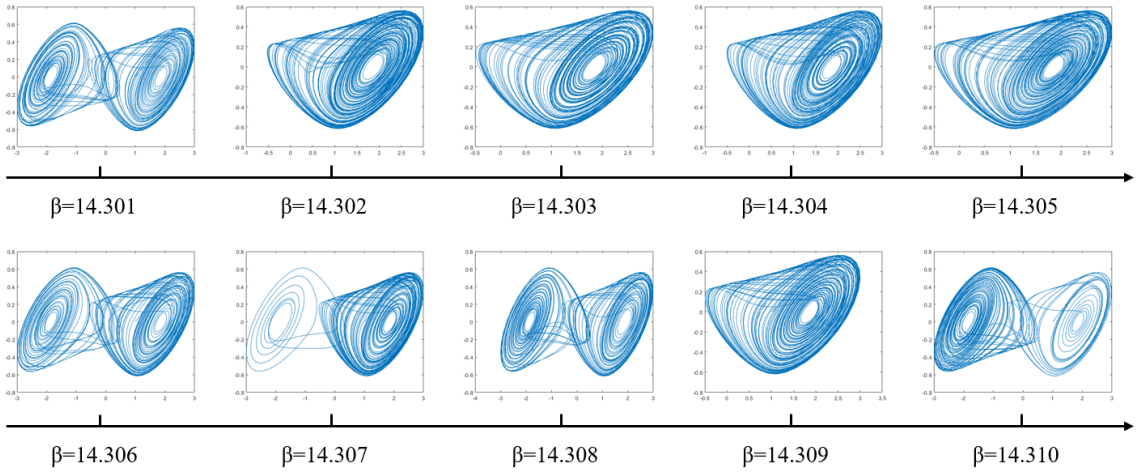

Fig. 15: $\beta \sim 10^{-3}$

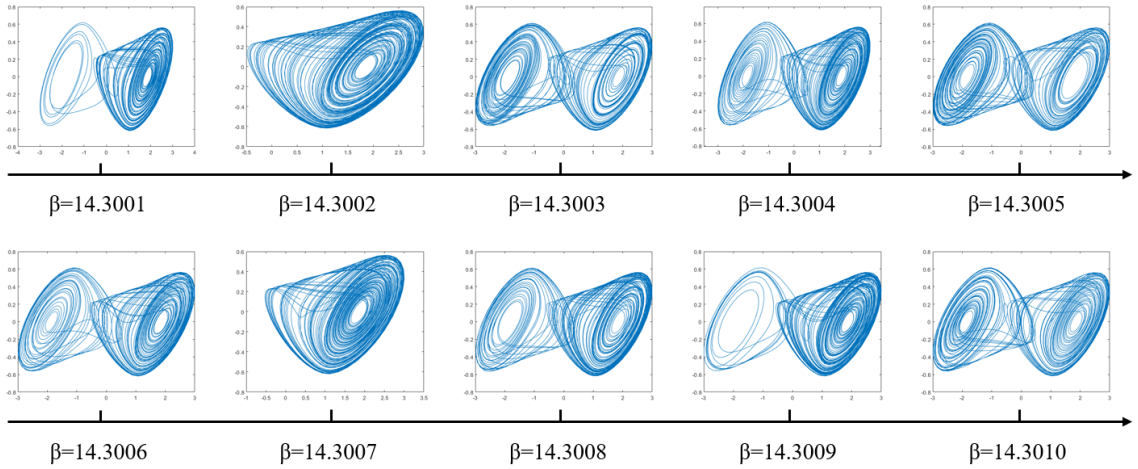

Fig. 16: $\beta \sim 10^{-4}$

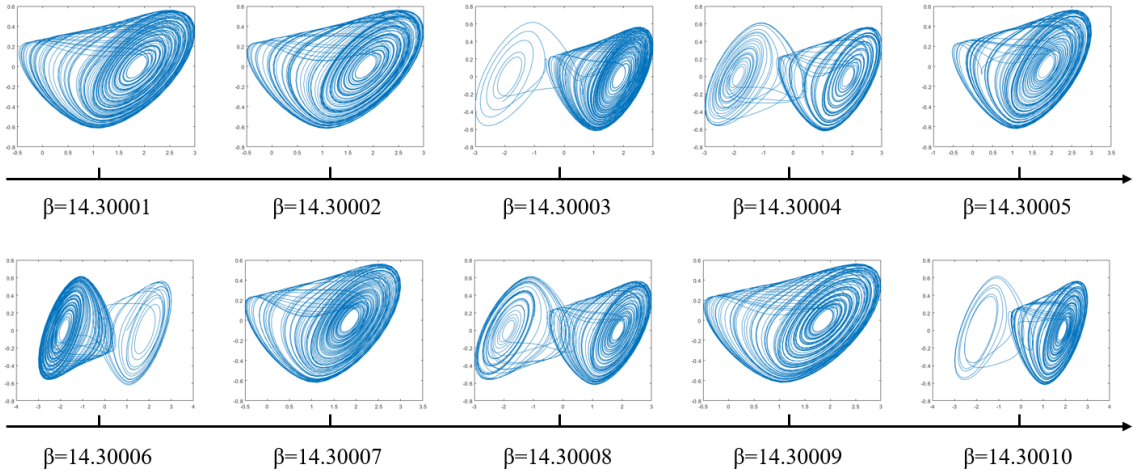

Fig. 17: $\beta \sim 10^{-5}$

We believe that this indicates that there seems to be some kind of self-similarity in the Chua's circuit. This conjecture comes from two considerations: (1) we observed the Lyapunov exponential spectrum of β in the Chua's circuit at different accuracies, and they all oscillate constantly up and down similar to Fig.5; (2) the geometry of the Tsai circuit double attractor in phase space seems to be of a fractional dimension, i.e., a fractal character with geometric structure, which is easily associated with self-similarity. Of course, the exact reasons for this need further research.

A.2 Simplification and derivation of circuit Eq.(5)

A simplified model of Eq.(5) can be derived, that has shown to still capture the dynamics qualitatively. First, the base currents $i_{B1,2}$ are assumed to be of negligible

influence. Second, we assume the current through R_3 does not load the collector of Q_1 down very much. Under these assumptions, $i_{B1,2} = 0$, $R3 \gg R1, R$, the system is adequately presented by

$$RC\frac{dv_1}{dt} = -v_1\left(1+\frac{R}{2R_1}\right) + v_2 + V_p\frac{R}{2R_1} - i_{C1}\frac{R}{2} \tag{8a}$$

$$RC\frac{dv_2}{dt} = -2v_2 + v_1 + v_{BE1} - i_{C2}R \tag{8b}$$

$$RC\frac{dv_{BE1}}{dt} = -v_{BE1} + v_2 \tag{8c}$$

$$R_3C_2\frac{dv_{BE2}}{dt} = -v_{BE2}\left(1+\frac{R_3}{R_4}\right) + \frac{v_1}{2} + \frac{V_p}{2} - i_{C1}\frac{R_1}{2} \tag{8d}$$

We use a strongly simplified and static piecewise linear transistor model:

$$i_{C1} = \begin{cases} \min\left(G_{M1}\left(v_{BE1}-V_{T1}\right), \frac{V_p+v_1}{R_1}\right) & , v_{BE1} > V_{T1} \\ 0 & , v_{BE1} < V_{T1} \end{cases} \tag{9a}$$

$$i_{C2} = \begin{cases} \min\left(G_{M2}\left(v_{BE2}-V_{T2}\right), \frac{v_2}{R_2}\right) & , v_{BE2} > V_{T2} \\ 0 & , v_{BE2} < V_{T2}. \end{cases} \tag{9b}$$

This transistor model shows three distinct regions, a cutoff region where $v_{BE} < V_T$, an active region where there is gain, and a saturated region. In this simplified model we set the threshold of conduction voltage $V_{T1,2}$ equal for both transistors at $V_T = 0.6\text{V}$. The collector saturation currents in Eq.(9) are chosen such that the collector to emitter voltages do not become negative. We set $G_{M1} = 16\text{mA/V}$ and $G_{M2} = 1\text{mA/V}$, corresponding with average transconductances.[20]

We nondimensionalize the system as follows

$$\begin{aligned} &x = \frac{v_1 - V_T}{V_T}, y = \frac{v_2 - V_T}{V_T}, z = \frac{v_{BE1} - V_T}{V_T}, u = \frac{v_{BE2} - V_T}{V_T}, t' = \frac{t}{RC}, \tau = \frac{R_3C_2}{RC} = 1.08, \\ &a = \frac{V_p}{V_T} = \frac{5}{0.6}, \quad b = 1 + \frac{R_3}{R_4}, \quad \alpha = G_{M1}R_1 = 80, \quad \beta = G_{M2}R = 10. \end{aligned} \tag{10}$$

This yields:

$$\begin{aligned} \dot{x} &= -2x - 1 + y + a - h_\alpha(z, 1 + a + x) \\ \dot{y} &= -2y + x + z - h_\beta(u, 2/3(y+1)) \\ \dot{z} &= -z + y \\ \tau\dot{u} &= -ub - b + \frac{a}{2} + \frac{1}{2} + \frac{x}{2} - \frac{1}{2}h_\alpha(z, 1 + a + x) \end{aligned} \tag{11}$$

where h is defined as:

$$h_\gamma(x, y) = \begin{cases} \min(\gamma x, y) & , x > 0 \\ 0 & , x \leq 0 \end{cases} \tag{12}$$

Appendix B Code for numerical calculation and drawing

B.1 Code for numerical calculation of normalized Chua's circuit

```
y0=[1;0;0];
tspan=[0,200];
[t,y]=ode45(@chua,tspan,y0);

plot3(y(:,1),y(:,2),y(:,3));
plot(y(:,1),y(:,2));
plot(y(:,1),y(:,3));
plot(y(:,2),y(:,3));

plot(1:length(y(:,1)),flip(y(:,1)));
hold;
plot(1:length(y(:,1)),flip(y(:,2)));
plot(1:length(y(:,1)),flip(y(:,3)));

x11 = ones(length(y(:,1)));
x01 = - ones(length(y(:,1)));
%plot(1:length(y(:,1)),x11(:,1),'black');
%plot(1:length(y(:,1)),x01(:,1),'black');

xlabel("time steps");
ylabel("x & y & z")
legend({'x','y','z'},"Location","best")

function dy_dt=chua(t,y)
m0=-1.2768;
m1=-0.6888;
a =8;
b =13.8;
dx_dt=a*(y(2)-y(1)-m1*y(1)-(m0-m1)*(abs(y(1)+1)-abs(y(1)-1))/2);
dy_dt=y(1)-y(2)+y(3);
dz_dt=-b*y(2);

dy_dt=[dx_dt;dy_dt;dz_dt];
end
```

B.2 Code for numerical calculation of normalized simple chaotic circuit

```
tspan=[0,400];
y0=[0;0;0.1;-0.5];
[t,y]=ode45(@simple,tspan,y0);

plot3(y(:,2),y(:,3),y(:,4));
plot(y(:,2),y(:,4));

function dy_dt = simple(t,y)
a = 5/0.6;
b =1.6818;
h_alpha = ((1+a+y(1))*(80*y(3)>(1+a+y(1)))+(80*y(3))*(80*y(3)<=(1+a+y(1))))*(y(3)>0);
h_beta  = (((y(2)+1)*2/3)*(10*y(4)>((y(2)+1)*2/3))+(10*y(4))*(10*y(4)<=((y(2)+1)*2/3))
    )*(y(4)>0);
dx_dt=-2*y(1)-1+y(2)+a-h_alpha;
dy_dt=-2*y(2)+y(1)+y(3)-h_beta;
dz_dt=-y(3)+y(2);
du_dt=-y(4)*b-b+a/2+1/2+y(1)/2-h_alpha/2;

dy_dt=[dx_dt;dy_dt;dz_dt;du_dt];
end
```

B.3 Code for calculating lyapunov exponent of Chua's circuit

```
Z=[];
m0=-1.2768;
m1=-0.6888;
a=8;
d0=1e-6;
bs = linspace(14.25,14.35,100);
transient = 50;
for b=bs
    params = [m0,m1,a,b];
    lsum=0;
    x=1;y=0;z=0;
    x1=1+d0;y1=0;z1=0;
    for i=1:100
        [T1,Y1]=ode45(@(t,X) chua(t,X,params),[0 1],[x;y;z]);
        [T2,Y2]=ode45(@(t,X) chua(t,X,params),[0 1],[x1;y1;z1]);
```

```
        n1=length(Y1);n2=length(Y2);
        x=Y1(n1,1);y=Y1(n1,2);z=Y1(n1,3);
        x1=Y2(n2,1);y1=Y2(n2,2);z1=Y2(n2,3);
        d1=sqrt((x-x1)^2+(y-y1)^2+(z-z1)^2);

        x1=x+(d0/d1)*(x1-x);
        y1=y+(d0/d1)*(y1-y);
        z1=z+(d0/d1)*(z1-z);

        if i> transient
            lsum=lsum+log(d1/d0);
        end
    end
    Z=[Z lsum/(i-transient)];
end
z00 = zeros(100);
plot(bs,Z);
%hold;
%plot(bs,z00,"r");
xlabel('beta'),ylabel('Largest Lyapunov Exponents');

function dX = chua(t,y,params)

m0 = params(1);
m1 = params(2);
a = params(3);
b = params(4);

dx_dt=a*(y(2)-y(1)-m1*y(1)-(m0-m1)*(abs(y(1)+1)-abs(y(1)-1))/2);
dy_dt=y(1)-y(2)+y(3);
dz_dt=-b*y(2);

dX=[dx_dt;dy_dt;dz_dt];
end
```

Appendix C Teacher's signature